Received: 18 October 2017 | Revised: 6 December 2017 | Accepted: 15 December 2017

DOI: 10.1002/fam.2505

RESEARCH ARTICLE

WILEY

Numerical evaluation of the flame to solid heat flux during poly(methyl methacrylate) combustion

A. Galgano[1] | C. Di Blasi[2,3] | C. Branca[1]

[1] Istituto di Ricerche sulla Combustione, C.N.R., P.le V. Tecchio, 80125 Napoli, Italy

[2] Dipartimento di Ingegneria Chimica, dei Materiali e della Produzione Industriale, Università degli Studi di Napoli Federico II, P.le V. Tecchio, 80125 Napoli, Italy

[3] IMAST—Distretto Tecnologico sull'Ingegneria dei Materiali Polimerici e Compositi e Strutture, P.zza Bovio 22, 80133 Napoli, Italy

Correspondence
C. Di Blasi, Dipartimento di Ingegneria Chimica, dei Materiali e della Produzione Industriale, Università degli Studi di Napoli Federico II, P.le V. Tecchio, 80125 Napoli, Italy.
Email: diblasi@unina.it

SUMMARY

The total net heat flux of the flame from a burning solid fuel is an important issue for the formulation of comprehensive solid-phase models useful for the fire testing of materials, but measurements are often affected by significant inaccuracy. In this study, an evaluation is conducted using a state-of-the-art model, coupling the descriptions of both gas- and solid-phase processes, for a thick poly(methyl methacrylate) slab burning in a cone calorimeter. It is observed that the total net heat flux (conductive and radiant flame heat fluxes minus surface reradiation losses) remains approximately constant (about 18 kW/m^2) as the intensity of the cone irradiance increases from 15 to 60 kW/m^2. The influences of some model assumptions and the solid degradation kinetics on this process variable are also assessed. Acceptable agreement is obtained between the predicted and the measured mass loss rates.

KEYWORDS

cone calorimeter, flame heat flux, modeling, PMMA combustion

1 | INTRODUCTION

The cone calorimeter,[1-4] based on the principle of oxygen depletion, is extensively used as an industrial standard for assessing material flammability. Its extensive use is due to the ability to determine a large number of fire properties in a single test by means of a small specimen. Properties include heat release rate, total heat release, time to ignition, time of sustained flaming, effective heat of combustion, smoke density, soot yield, mass loss rate, and yields of CO, CO_2, and other combustion products. Only the flame spread rate cannot be directly determined. The heat source is an electrical coil, shaped like a truncated hollow cone, which ensures a uniform heat flux over the exposed surface and a nearly 1-dimensional heat transfer across the specimen, where bottom and edge effects are minimized. Both piloted and spontaneous ignition can be established. Owing to the well-defined heating conditions, cone calorimeter data can also be useful for the experimental validation of mathematical models.

Nomenclature: A, pre-exponential factor, s^{-1}; E, activation energy, kJ/mol; L, sample thickness, m; $\dot{m}$, MMA mass flow rate, g/m^{2}s; Q, heat flux, W/m^2; T, temperature, K; t, time, s; v, velocity, m/s; X, polymer conversion level

Subscripts: 0, nominal value; 50, polymer conversion of 50%; av, average value in gas phase; c, polymer conversion of 95%; cond, conductive; cone, cone calorimeter; max, maximum value in gas phase; N, net flux (total); Nf, net flux due to flame; rad, radiative; re-rad, reradiative; s, surface of PMMA sample; TC, limit temperature for radiation absorption of MMA

Different approaches have been used to describe solid fuel combustion in a cone calorimeter. The simplest one consists of thermokinetic models for the solid-phase processes only,[5-12] where the effects of the heat flux from the flame are either completely neglected, as quantitative comparison with the measurements is not made, or are taken into account by means of a guessed constant value. Then, to obtain the heat release rate for a generic material, the mass loss rate is multiplied by the heat of combustion. The absence or extremely approximate description of the gas-phase processes is certainly a weak point for this category of models, but they generally provide accurate descriptions of the processes taking place in the solid phase that play a crucial role in the predicted evolution of the heat release rate. A significant effort has been made[8] to compare predicted and measured heat release rates for 3 thermoplastic polymers for widely variable heating conditions, but it is evident that further work is still needed to develop a truly predictive model even for this class of relatively simple materials. In fact, the flame heat flux is simply estimated by fitting the cone calorimeter heat release rate for a single external irradiance level. Quantitative predictions are improved when using heating curves specific of each irradiation level.[13] On the other hand, the flame heat fluxes seem to depend not only on the specific material properties but also on the estimation method (for instance, 10 kW/m^2 [Patel et al[10]], 11-15 kW/m^2 [Stoliarov et al[8] and Patel et al[10]], or 16-47 kW/m^2 [Spearpoint and Quintiere[7]]). Hence, this is an aspect that deserves further careful study.

The positive side of solid-phase models is that, given the relatively small number of partial differential equations and the acceptable approximation of 1-dimensional behavior of the solid, a numerical solution can be easily implemented and the computational times are very modest. In contrast with this treatment, multidimensional equations for the gas-phase processes, adjacent the solid, have also been formulated to describe ignition[14] and burning.[15,16] However, being the main emphasis on the description of the gas phase, highly simplified descriptions are applied of the processes taking place in the solid phase. This is clearly a weak point and, in general, the computational effort is large. Moreover, the quantitative assessment of the models is limited only to the ignition stage,[14] and they are not applied to conduct evaluations of the flame heat flux and to assess the role of important parameters on the process characteristics.

A compromise between these 2 categories is represented by models, which couple detailed descriptions of the solid-phase processes with simplified treatments of the gas phase as 0- or 1-dimensional.[17,18] However, the assumptions made by these models are valid only in preignition and immediate postignition region and cannot be applied to predict the burning stage of the material.

This study represents a further contribution about the determination of the flame heat flux for solid burning in a cone calorimeter based on numerical simulation results. The model consists of a 2-dimensional computational fluid dynamics model for the gas phase coupled with a 1-dimensional detailed model for the solid phase, applied to the combustion of thick poly(methylmethacrylate) (PMMA) samples. To support the validity of the predictions, the model is experimentally validated. Also, a parametric analysis is conducted aimed at evaluating the impact of model assumptions/parameters on the process predictions, in particular, the flame heat flux.

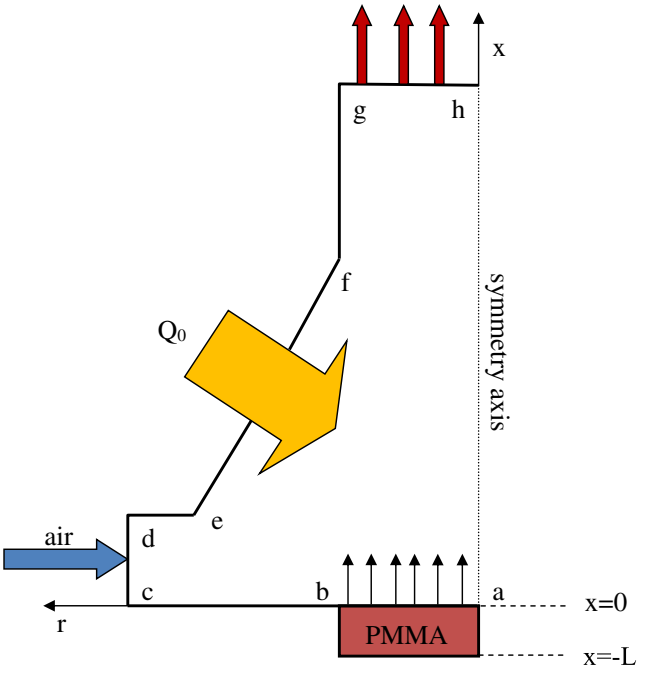

FIGURE 1 Schematic of the modeled cone calorimeter (ab = 5 cm, bc = 5 cm, cd = 2.5 cm, de = 2 cm, ef = 8 cm, fg = 4.8 cm, gh = 4 cm, ha = 14 cm) and solid sample (PMMA) with thickness L [Colour figure can be viewed at wileyonlinelibrary.com]

2 | MATHEMATICAL DESCRIPTION

Poly(methylmethacrylate) has often been used as a reference material in cone calorimeter combustion[19-23] to evaluate material flammability. The problem described by the mathematical model considers the conditions of a standard cone calorimeter test, according to the schematic of the problem reported in Figure 1, for a thick sample, including both the solid and gas phases.

Solid-phase processes are described following the treatment proposed in previous models of this research group for PMMA decomposition.[24,25] In brief, the unsteady mass and energy conservation equations are formulated for a 1-dimensional approximation (axial direction), combined with endothermic decomposition kinetics of PMMA to give the vapor-phase monomer methylmethacrylate (MMA), showing a linear dependence on the polymer density and an Arrhenius dependence on temperature, a surface regression proportional to the amount of degraded polymer, a condensed-phase radiation absorption according to the Beer law and local thermal equilibrium between the phases.

The FLUENT software[26] is chosen for the simulation of the gas-phase processes, because of its ability to describe the multidimensional turbulent reactive flows, specifying the k-ε model for mildly turbulent flows, the global combustion kinetics in accordance with the Eddy Dissipation Concept, the discrete transfer radiation model for the radiative heat exchanges, the single-step model for soot formation, and radiation absorption models for the combustion products (carbon dioxide, water, and soot), and the vapor-phase MMA including a dependence on temperature and concentration.[27,28] However, given that for sufficiently high temperatures, MMA decomposes to give methanol, methane, propylene, 2-methylpropylene, acetone, formaldehyde, and methyl pyruvate,[29] it is assumed to absorb radiation only until a limit temperature, T_{TC}, is reached. Finally, as in previous studies of solid fuel combustion,[30-32] it is assumed that the gas phase is in a steady state with respect to the unsteady solid phase (this assumption is justified by the much shorter characteristic times of the gas phase with respect to those of the solid phase) and its size remains constant (the surface regression is compensated by an upward displacement of the sample).

The coupling between the gas and solid phases occurs at the surface of the sample by means of the boundary conditions. It should be recalled that an iterative computational procedure is required because the heat flux generated from the flame is not known a priori. In the first step, the solid-phase variables are computed assuming that the total heat flux coincides with that of the cone. Then, with the aid of the solid-phase solution at the solid/gas interface, the gas-phase solution is obtained, including the flame heat flux. At this point, the solid-phase variables need again to be evaluated taking into account that the heat flux consists of that emitted by the cone with the additional (positive) contribution, for times longer than the ignition time, of the conductive and radiative heat flux of the flame and the (negative) surface reradiation loss. However, the modified heating conditions of the solid also affect the gas phase via, for instance, the surface temperature and

volatile mass flux. Therefore, the solution procedure is iterated until a convergent solution is achieved that, among others, leads a constant value of the flame heat flux.

The coupling between the 1-dimensional model of the solid phase and the 2-dimensional model of the gas phase is accomplished assuming flat radial profiles of the surface temperature and the monomer efflux rate and average values of the flame heat fluxes. The average values refer to the inner part of the sample to avoid inaccurate estimation at the edges induced by models of different dimensionality. The conductive heat flux is computed with reference to the control volumes adjacent the surface assuming a second-order polynomial and a laminar thermal conductivity based on the low efflux velocity of the monomer.

It is beyond doubt that a multidimensional treatment of the solid phase would be more realistic, and this is certainly one of the features that should be taken into account in the future for the development of more advanced models. However, apart from the simplicity of the 1-dimensional formulation and the reduced computational effort, the proposed model, as shown in the following, produces acceptable quantitative predictions, without any adjustable parameter. This is certainly a point in favor of the goodness of the approach from the practical point of view. Moreover, it should be mentioned that this approach also suffices to capture the salient features of the process in the prediction of wood log burning.[32,33] In fact, it has been observed to give rise to small deviations with respect the corresponding 2-dimensional formulation. The solid mass fraction is approximately the same for more than half the process time and the overestimation reaches a maximum of about 12% at near-complete conversion. Moreover, the conversion time is overestimated by 9% implying that the net heat flux from the flame is anyway only slightly underestimated.

It is also worth recalling that approximate theories generally introduce, apart from radiation, a conductive gas-phase heat flux based on an empirical coefficient and an engineering evaluation of the temperature difference that, when both the solid- and gas-phase processes are mathematically described, there is no need to introduce. On the other hand, at the surface, the pure convective contribution coincides with the heat transported by the vapor-phase fuel.

Another aspect that should be given consideration is the unsteady character of solid fuel degradation and consequently the coupled gas-phase combustion. In principle, the iterative solution procedure for the 2 phases should be dynamic, that is, applied for several successive times, starting from preheating followed by ignition, combustion, and quenching. However, for thermally thick samples, the initial and final transients correspond to a very small part of the duration of the process that occurs under quasi-steady conditions.[4,24,25] Therefore, it is expected that the selection of a quasi-steady configuration of the solid, for coupling with the gas phase, is effective and accurate for the entire duration of process. More specifically, as shown in the following, it has been found a dynamic coupling of the 2 phases gives rise to coincident results with a steady coupling considering conditions of solid conversion of 50%. In the case of dynamic coupling, the process simulation is started from the ignition time, without taking into account, for the solution of the solid-phase model, the absorbance of radiation by the vapor-phase monomer during the preignition period.

3 | RESULTS

The schematic of the problem, reported in Figure 1, also includes the relevant sizes of interest for the cone calorimeter. Similar to the experiments performed by Luche et al,[23] the sample shows a 1.4-cm thickness and 5-cm half width and a density of 1213 kg/m^3. The numerical approximation foresees 11 700 and 200 control volumes for the gas and solid phases, respectively. The input data for the numerical simulations are derived from previous literature, without any adjustable parameter. They are briefly examined below.

For the solid-phase model, the input parameters are essentially those already used[24,25] for PMMA thermal decomposition. Moreover, as for the validation of the model the experiments for black PMMA[23] are used, the polymer absorption properties and the surface emissivity are specific of this material (a solid-phase radiation absorption coefficient[34] of 2620 m^{-1} and a surface emissivity[35] of 0.945). Also, the PMMA decomposition kinetics previously evaluated[24] is used (parameters practically coincide with those reported in Stoliarov et al[8]). However, it should be noticed that both physical and chemical properties of PMMA are dependent on the production process and product specifications/applications. In particular, it has been recently observed[36] that the decomposition kinetics is highly affected by the polymerization degree in relation not only to the parameter values but also to the reaction mechanism (eg, number of reactions steps) with consequent remarkable influences on the fire behavior.

The exposure of the sample to an assigned irradiation level is achieved by means of the calculation of the adequate cone wall temperature (the wall emissivity[37] is taken equal to 0.55). For instance, a temperature of the conical heater, T_{cone}, equal to 1043 K results in a radiant heat flux, Q_0, of 50 kW/m^2 at the start of the test. This temperature is very close to the value of 1030 K observed[13] for the standard vertical distance of the sample to the cone heater, which is an important parameter for the definition of the actual heat flux reaching the sample surface.[4] Given the schematization of the cone, the inlet boundary requires the assignation of the air velocity. Following the measurements and the analysis conducted in Tsai et al,[14] an average velocity of 0.24 m/s is imposed at the d-c section. The global combustion kinetics of MMA vapors takes place with the parameters reported in Tsai et al[14] and reaction enthalpy as Di Blasi et al.[18] Following Zeng et al,[29] the limit temperature, T_{TC}, for radiation absorption by the MMA vapors is taken equal to 773 K. Furthermore, as anticipated, to avoid inaccuracies originated from coupling models of different dimensionality, the flame heat fluxes are evaluated only over a width of 3 cm with respect to the total half width of the sample equal to 5 cm. In fact, the 1-dimensional approximation of the solid-phase model does not allow the details of the edge zones to be accurately predicted. In this way, the introduction of unpredictable errors in the computational procedure is avoided. Finally, when a dynamic coupling between the 2 phases is made, the ignition times are those measured.[23]

Numerical simulations are preliminarily made to illustrate the main features of the combustion process and to demonstrate the validity of the model assumption based on a 50% solid-phase conversion for the evaluation of the flame heat flux (iterative coupling between the 2 phases, including the effects of the unsteady character of solid

degradation) for a cone irradiation level of 50 kW/m^2. Then, this operating variable is varied in the range 15 to 60 kW/m^2 to assess its influences on the flame heat flux and to compare predicted and measured rates of polymer weight loss. Also, a parametric analysis is made about the effects of the kinetics of solid degradation on the total net flame heat flux.

3.1 | PMMA combustion characteristics

In this section, the characteristics of PMMA combustion are discussed for a cone irradiance Q_0 = 50 kW/m^2, which is considered as the reference case (together with the assumptions and the parameter values summarized above). The model performances in relation to convergent coupling between the solid and gas phases can be evaluated from Table 1 listing the main output variables for the solid phase (t_{50}, the time to achieve a PMMA conversion of 50% and the corresponding surface temperature, T_s, and monomer efflux rate, v_s, and the conversion time, t_c, corresponding to a PMMA conversion of 95%) and the gas phase (the conductive heat flux, Q_{cond}, the flame radiative heat flux, Q_{rad}, the heat flux reradiated from the surface, $Q_{re\text{-}rad}$, the total net heat flux of the flame, Q_{Nf}, the total net heat flux (including the radiation emitted by the cone), Q_N, the average and maximum temperatures, T_{av} and T_{max}) for 3 consecutive iterations (each iteration consists of the sequential solution of the solid- and gas-phase models). Figure 2 reports the solid mass loss rate and the surface temperature versus time for the first (I), second (II), and third (III) iterations. It appears that the differences between the variables for the first 2 iterations are not negligible. Instead, they become negligible for all the variables between the second and third iterations (maximum differences around 4%). Therefore, it can be stated that 2 iterations are sufficient to achieve a convergent solution. The evaluation of the flame heat fluxes is particularly useful because experimental approaches are often not accurate[19]; nevertheless, this information is needed, as input, for the solid-phase combustion models. The total net heat flux increases from the nominal value of 50 kW/m^2 to about 67.5 kW/m^2, with a global net contribution from the reactive gas phase around 17.5 kW/m^2, consisting of the sum of radiative (22.5 kW/m^2) and conductive (7.0 kW/m^2) heat fluxes of the flame subtracted by surface reradiative losses (12 kW/m^2). Tough, as expected, the radiative and reradiative terms are quantitatively the most important, the conductive term also is significant (about 65% of net additional radiative contribution). The additional net heat flux causes a diminution in the PMMA conversion time (by about 26%) and an increase in the v_s value (by about 40%)

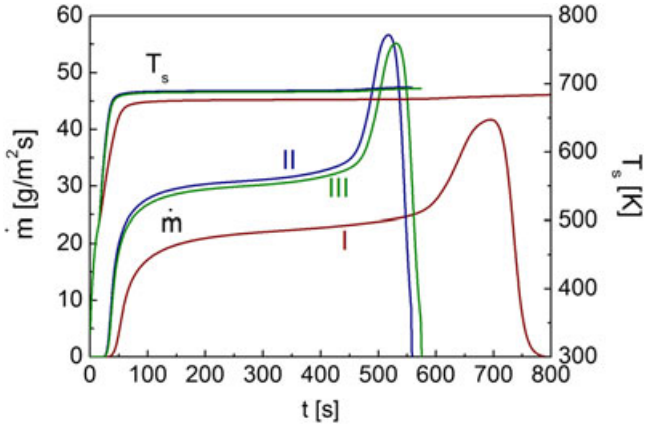

FIGURE 2 Poly(methylmethacrylate) mass loss rate and surface temperature versus time as simulated for the reference case (Q_0 = 50 kW/m^2) and 3 successive iterations: I ($Q_N = Q_0$), II (Q_N = 69.1 kW/m^2), and III (Q_N = 67.2 kW/m^2) [Colour figure can be viewed at wileyonlinelibrary.com]

and the surface temperature T_s (from about 677 to 689 K). As stated above, the flame heat flux contributions are evaluated over the inner part of the sample but it is useful to observe that the actual values along the radial direction vary from about 5 to 18 kW/m^2 (conductive contribution) and from 20 to 27 kW/m^2 (radiative contribution).

The time profiles of the surface temperature and the polymer mass loss rate own the typical shapes observed or simulated for thick thermoplastic materials.[4,23-25] In particular, the mass loss rate shows 4 main zones corresponding to a short period of rapid rise, a plateau with approximately constant rate, the attainment of the peak rate, and finally a decay zone.

The convergent solution for the gas phase is shown by the color maps of the temperature and the mass fractions of chemical species, including soot, reported in Figure 3A-G. Figure 4 shows the corresponding vector velocity field. The thermal plume is attached at the edges of the specimen and clearly extends above the integration domain considered by the model, with a shape reproducing the experimental evidence.[19] Temperatures vary from those of the ambient air and the relatively low surface value up to a maximum around 1860 K. A thin diffusion flame is established, which separates a fuel-rich central zone from an oxygen-rich lateral zone. The flow field puts into evidence the fuel inlet from the surface and the double lateral inlet of air, with maximum velocities reached at the exit (value around 4.0 m/s).

TABLE 1 Predicted output variables: t_{50} is the time to achieve a PMMA conversion of 50% (with the corresponding surface temperature, T_s, and monomer efflux rate, v_s), t_c, the conversion time (PMMA conversion of 95%), Q_{cond} and Q_{rad}, the flame conductive and radiative heat fluxes, $Q_{re\text{-}rad}$, the heat flux reradiated from the surface, $Q_{Nf} = Q_{cond} + Q_{rad} - Q_{re\text{-}rad}$, the net heat flux of the flame, Q_N, the net (total) heat flux (including the radiation emitted by the cone), Q_{Nf}/Q_0, the percentage variation in the net heat flux of the flame with respect to the nominal heat flux emitted by the cone, and T_{av} and T_{max}, the average and maximum temperatures of the gas phase for the reference case (Q_0 = 50 kW/m^2) and 3 successive iterations: I ($Q_N = Q_0$), II (Q_N = 69.1 kW/m^2), III (Q_N = 67.2 kW/m^2)

Iterations	t_{50}, s	T_s, K	v_s, cm/s	t_{max}, s	v_{smax}, m/s	t_c, s	Q_{rad}, kW/m^2	Q_{cond}, kW/m^2	$Q_{re\text{-}rad}$, kW/m^2	Q_N, kW/m^2	Q_{Nf}, kW/m^2	100 × Q_{Nf} / Q_0	T_{av}, K	T_{max}, K
I	465	677	1.6	696	3.0	718	21.5	8.8	11.3	69.1	19.1	38.2	704	1855
II	332	690	2.3	518	4.1	532	22.6	6.7	12.2	67.2	17.2	34.4	720	1859
III	342	689	2.2	532	4.0	546	22.5	7.0	12.0	67.5	17.5	35.0	717	1862

To take into account the initial and final transients of the solid phase, a dynamic coupling procedure is also implemented. It consists of the application of the iterative procedure already illustrated for a number of conditions (ie, polymer conversion levels, X), which span the entire time interval of polymer decomposition. Thirteen consecutive times are considered, as reported in Table 2, which refers to a convergent solution again reached at the second iteration. Owing to the steady gas phase, the preheating stage is not modeled but the first condition examined refers to the ignition condition. Figure 5 compares the convergent solution for the mass loss rate, the surface temperature, and the total net heat flux as functions of time for the reference case, as simulated for the steady coupling (conditions of 50% PMMA conversion) and the dynamic coupling. Apart from the obvious differences at very short (near to ignition) and very long (near to burn out) times, the 2 solutions are approximately the same, testifying the good accuracy of the treatment proposed.

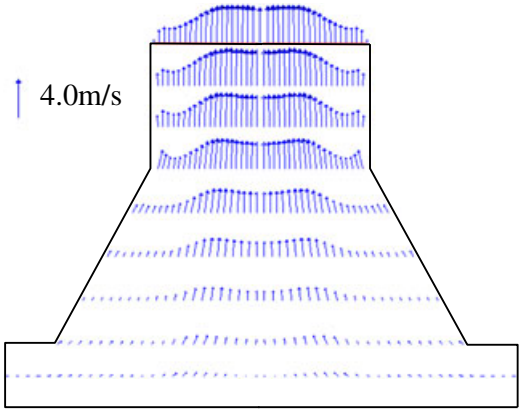

FIGURE 4 Gas-phase vector velocity field as predicted for the reference case (Q_0 = 50 kW/m^2) [Colour figure can be viewed at wileyonlinelibrary.com]

3.2 | Effects of the cone irradiance

The analysis about the effects of the cone radiative heat flux is made for Q_0 values of 15 to 60 kW/m^2, which correspond to cone temperatures in the range 775 to 1092 K. Figure 6A,B report the color maps of the gas-phase temperature and the monomer mass fraction for radiative heat fluxes emitted by the cone, Q_0, of 15 and 60 kW/m^2. Also, the conductive and radiative flame heat fluxes, the surface heat losses, the net heat flux of the flame, the percentage variation in the net heat flux with respect to the heat flux emitted by the cone and the other process variables are reported versus the nominal heat flux emitted by the cone, Q_0, in Figures 7A,B. As expected, the characteristic temperatures and the monomer efflux rates increase with Q_0. For the range of external heat fluxes examined, the percentage variations are the highest for the average gas temperature (about 14% versus approximately 1% for the maximum gas temperature and 3% for the surface temperature), as a consequence of the modified shape of the flame (leading edge and thermal plume). The influence of Q_0 on the surface heat losses and the flame radiative heat flux is small, corresponding to values in the range 11 to 12 and 21 to 23 kW/m^2, respectively, as expected from

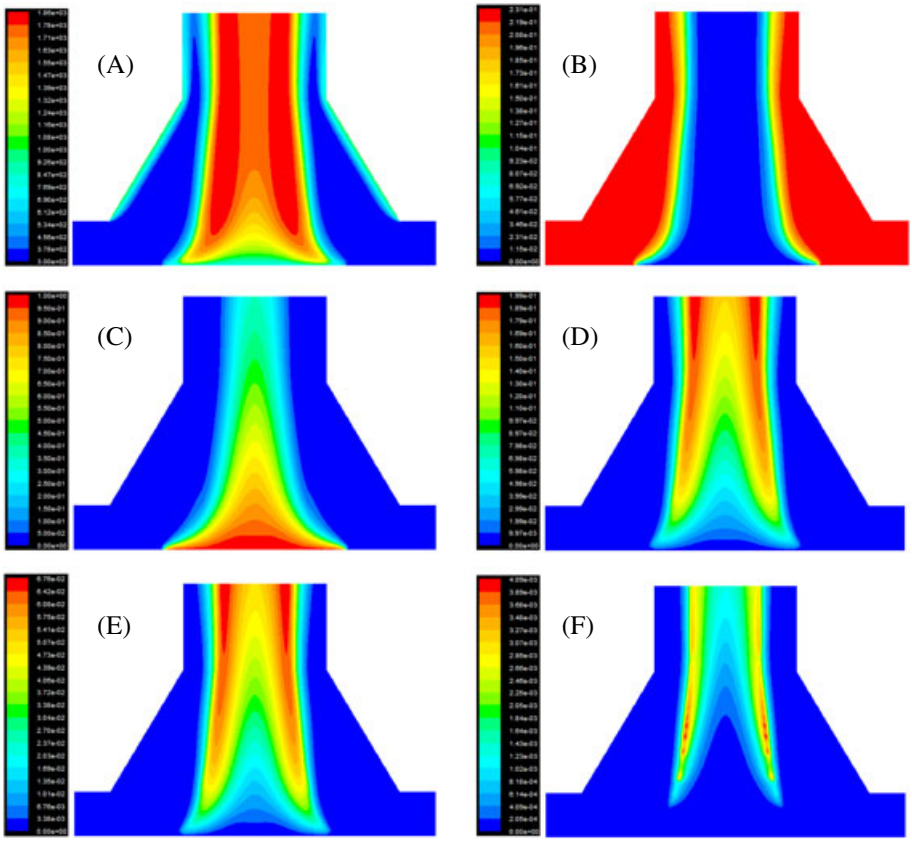

FIGURE 3 Color maps of the gas temperature (A) and the mass fractions of oxygen (B), MMA vapors (C), CO_2 (D), H_2O (E) and soot (F), as predicted for the reference case (Q_0 = 50kW/m_2) [Colour figure can be viewed at wileyonlinelibrary.com]

TABLE 2 Predicted output variables for the solid phase and the gas phase (for the definitions see Table 1) for the reference case (Q_0 = 50 kW/m^2) and a dynamic coupling referred to times between 17.4 s (ignition time) and 545 s (conversion time) (X is the polymer conversion level)

t, s	X	T_s, K	v_s, cm/s	Q_{rad}, kW/m^2	Q_{cond}, kW/m^2	$Q_{re\text{-}rad}$, kW/m^2	Q_N, kW/m^2	Q_{Nf}, kW/m^2	100 × Q_{Nf} / Q_0	T_{av}, K	T_{max}, K
17.4	2.5×10^{-3}	501	5.0×10^{-6}	9.4	14.4	3.4	70.4	20.4	40.8	633	1852
35	4.0×10^{-3}	673	0.6	21.8	13.1	11.0	73.8	23.8	47.6	678	1832
43	0.01	683	1.2	20.9	10.5	11.6	69.8	19.8	39.6	696	1841
105	0.10	688	2.0	22.0	7.8	12.0	67.8	17.8	35.6	712	1855
164	0.20	688	2.1	22.1	7.5	12.0	67.6	17.6	35.2	712	1853
222	0.30	689	2.2	22.5	7.0	12.0	67.5	17.5	35.0	716	1862
278	0.40	689	2.2	22.5	7.0	12.0	67.5	17.5	35.0	717	1862
335	0.50	689	2.2	22.5	7.0	12.0	67.5	17.5	35.0	716	1862
390	0.60	689	2.2	22.5	7.0	12.0	67.5	17.5	35.0	717	1862
443	0.70	689	2.4	22.2	6.9	12.0	67.1	17.1	34.2	720	1856
493	0.80	689	2.9	21.8	5.4	12.1	65.1	15.1	30.2	728	1858
529	0.90	690	3.7	21.0	4.5	12.1	63.4	13.4	26.8	746	1876
545	0.95	692	3.4	19.5	4.9	12.3	62.1	12.1	24.2	740	1865

the mild variations on the surface temperatures and monomer mass flux rates. The conductive term exhibits values in the range 9 to 6 kW/m^2, as Q_0 is increased, most likely owing to an increasing distance of the flame from the degrading surface.

Based on these figures, it can be stated that the total net flux of the flame only weakly varies (19-17 kW/m^2) as the cone irradiance level is varied (range 15-60 kW/m^2) and, from an engineering point of view, a constant value (18 kW/m^2) can be assumed. It is interesting to notice that, for low Q_0 (below 20-25 kW/m^2), the radiative contribution of the flame is quantitatively more important than that of the cone. To explain this result, it should be taken into account that the concentration of the vapor-phase monomer, as well as the amount of absorbed radiation, increases with Q_0. As a consequence, the total net heat flux, associated with the presence of the gas-phase combustion, becomes a successively smaller percentage of the applied heat flux. In quantitative terms, for the range of cone irradiance fluxes considered, it varies from about 127% to 28%. This result is in qualitative agreement with the measurements[13] for poly(butylene terephtalate) combustion in a cone calorimeter, where the percentage of increase of the total incident heat flux varies from about 38% to 6% for cone irradiances from 35 to 70 kW/m^2.

In agreement with experimental observation,[38] the production of vapor-phase species from solid decomposition introduces significant attenuation in the radiation that actually reaches the solid surface. The attenuation becomes successively more important as the intensity of the external heat flux is increased as a consequence of the increased concentration of the vapor-phase fuel. Moreover, while in the preignition period, the gas-phase temperature is relatively low and it is not likely that the monomer undergoes decomposition, in combustion,

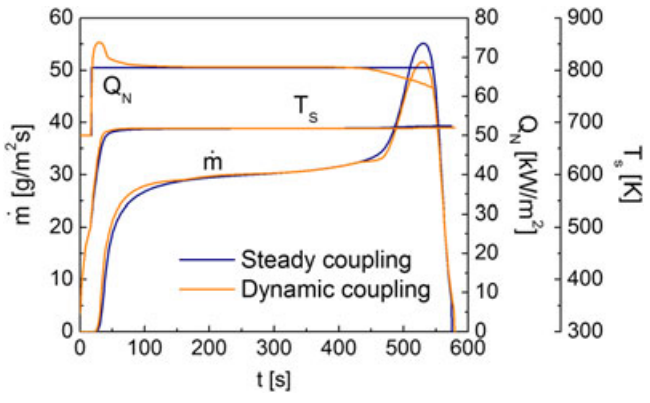

FIGURE 5 Poly(methylmethacrylate) mass loss rate, surface temperature, and net (total) heat flux, Q_N, versus time as simulated for the reference case (Q_0 = 50 kW/m^2) with steady and dynamic coupling between the solid- and gas-phase models [Colour figure can be viewed at wileyonlinelibrary.com]

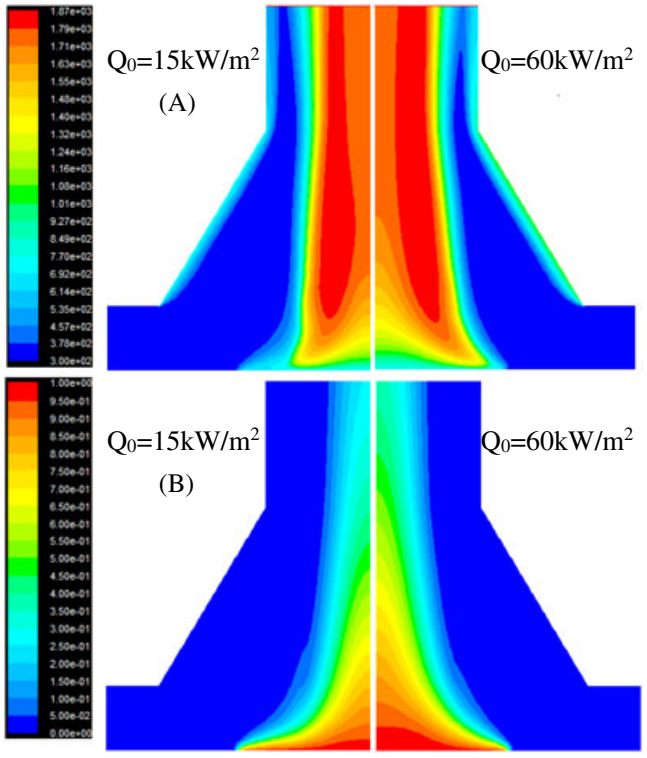

FIGURE 6 Color maps of the gas temperature (A) and the mass fractions of MMA vapors (B) as predicted for cone heat fluxes, Q_0, of 15 and 60 kW/m^2 [Colour figure can be viewed at wileyonlinelibrary.com]

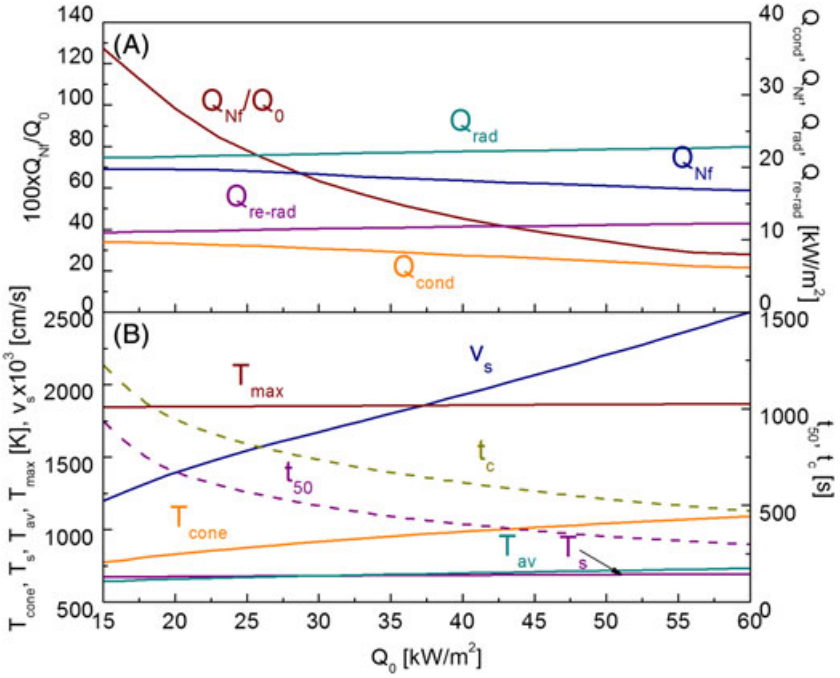

FIGURE 7 A,B, Predicted output variables: t_{50} is the time to achieve a PMMA conversion of 50% (with the corresponding surface temperature, T_s, and monomer efflux rate, v_s), t_c, the conversion time (PMMA conversion of 95%; Q_{cond} and Q_{rad}, the flame conductive and radiative heat fluxes, respectively; $Q_{re\text{-}rad}$, the heat flux reradiated from the surface; $Q_{Nf} = Q_{cond} + Q_{rad} - Q_{re\text{-}rad}$, the net heat flux of the flame; Q_{Nf} / Q_0, the percentage variation in the net heat flux of the flame with respect to the nominal heat flux emitted by the cone; T_{av} and T_{max}, the average and maximum temperatures of the gas phase, respectively; and temperature of the cone wall, T_{cone}, versus the heat flux emitted by the cone, Q_0 [Colour figure can be viewed at wileyonlinelibrary.com]

decomposition is an important chemical process and, in this way, the radiation absorption may consequently change. In reality, the contribution of each species is greatly dependent on its thermal conditions. As indicated by simulations carried out for Q_0 = 50 kW/m^2, the combustion products (CO_2, H_2O, and soot), that are formed at high temperature, globally emit radiation, with a radiative flame heat flux that, in the absence of the fuel contribution, reaches a value around 27 kW/m^2. In the absence of soot absorption, this value lowers to about 23 kW/m^2 (versus 22 kW/m^2 of the reference case). On the contrary, the monomer, which is formed at relatively low temperatures and becomes transparent for temperatures above 773 K, actually absorbs thermal radiation.

On the whole, it can be stated that, as already reported in previous studies,[8,20,21,23] the net heat flux from the flame remains approximately constant as Q_0 is varied. In particular, the constancy was attributed[21] to the shape of the flame for materials burning in the cone calorimeter (ratio of the height to the diameter above 2) exhibiting a constant emissivity with a small convective contribution. Moreover, from the quantitative point of view, the computed net heat fluxes (average value around 18 kW/m^2) are comparable to those estimated in previous literature. Data, for black PMMA, range from a total value of 37 kW/m^2 (Rhodes and Quintiere[20]), with a corresponding net contribution of 28 kW/m^2 (Hopkins and Quintiere[21]), or 20 kW/m^2 (Beaulieu and Dembsey[39]) to 17.7 kW/m^2 (Luche et al[23]), with a corresponding net contribution of 14.9 kW/m^2 (also, a net contribution of 12 kW/m^2 is reported for translucent PMMA[8]). In general, the differences can be attributed to the experimental uncertainties, the cone design and the sample position, the sample properties and the result interpretation. It has also been put into evidence[8] that the flame heat flux (and total heat released), for sooting flames, may depend on the imposed irradiance level. Indeed, the flame heat flux increases through the reradiation of energy from the soot particles back to the burning sample. It is also interesting to observe that the heat fluxes evaluated here are comparable to those reported[40] for the steady burning of vertical slabs of translucent PMMA. Indeed, depending on the sample height, the total flame heat flux varies approximately in the range 23 to 31 kW/m^2 with surface reradiation equal to 11.5 kW/m^2.

3.3 | Experimental validation

The mass loss rate curves preserve the same shape, with the presence of several zones already discussed above, independently from the external irradiance level, as shown in Figure 8 where the model predictions are compared with the measurements.[23] For both cases, the duration of the various zones depends on the external heating conditions. More specifically, as the cone irradiance level is increased, the duration of the plateau is progressively reduced until the shape of the mass loss curve tends to assume the same qualitative features shown by thermally thin samples.[4] Hence, it can be anticipated that, for very high heat fluxes, the quasi-steady coupling between solid and gas phases may be not anymore valid and the computationally more laborious dynamic coupling should be used. The quantitative agreement between predictions and measurements is acceptable, except for the final slow decomposition period observed in the experiments. This corresponds to the consumption of the residual PMMA sample in the holder and is also visible in the heat release rate curves, although the duration/magnitude is quantitatively different, because of the differences in the characteristic times of the solid (mass loss rate) and gas (heat release rate) phases. It is important to point out that this is peculiar of the combustion process as the mass loss rates curves measured and predicted during the anaerobic gasification tests[24,25,41] present a rapid decay soon after peaking. More precisely, the slow combustion zone is considered to be caused by the burning of the material located under the lip of the edge of the sample holder.[8] Moreover, for this last stage, it is likely that the cone irradiance concerns a smaller surface area, so that the heat flux actually reaching the sample

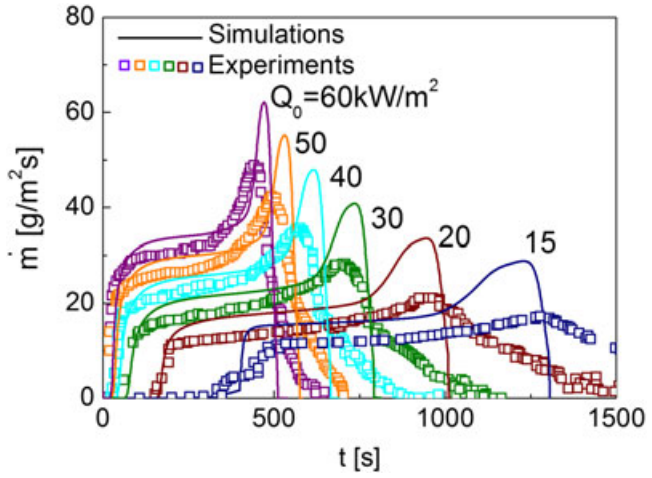

FIGURE 8 Poly(methylmethacrylate) mass loss rate as simulated in this study (solid lines) and measured by Luche et al[23] (symbols) versus time for nominal heat fluxes emitted by the cone, Q_0, in the range 15 to 60 kW/m^2 [Colour figure can be viewed at wileyonlinelibrary.com]

is reduced with respect to the nominal value.[8] These features cannot be captured by the 1-dimensional solid-phase model used here.

The information, based on the visual observation of the process during the four stages of the mass loss curves,[23] is also important for explaining the other small differences between predictions and measurements. The time periods, immediately preceding and following ignition, are associated with intense bubbling, but this phenomenon is not described by the model. It influences heat and mass transfer rates across the polymer and, in this way, the mass loss rate.[42] The plateau appears to be associated with sample swelling, which reduces the heat transfer rate through the solid and makes longer the conversion time.[42,43] This feature is also disregarded by the model. Another source of discrepancy between model and experiments can be found in the deviations from the assumptions of a constant value of the heat flux emitted by the cone.[4] Indeed, the emitted radiation decreases as the sample distance is increased, which is unavoidable during conversion and whose effects are especially important for large thicknesses. The repeatability of the cone measurements may also be critical as, even for the simplest polymers (ie, PMMA), the difference in the peak of the heat release rate and corresponding time may reach about 20%.[8] Finally, as shown in the following, the decomposition kinetics, not specific of the PMMA samples used in the experiments, may also play a role. However, on the whole, the agreement between predictions and measurements can be considered acceptable.

3.4 | Effects of the solid degradation kinetics

The degradation of thermoplastic materials in inert atmosphere is largely influenced by the kinetic law. In fact, the reported variation range of the 2 parameters, pre-exponential factor and activation energy, is rather wide, depending on the polymerization process.[44] Hence, to examine the influence of the degradation kinetics on the combustion process, the data from various authors[45-48] cited in the review[44] are compared with the reference values[24] of this study. Table 3 reports the main solid and gas-phase outputs (with the corresponding couples of kinetic parameters used for the simulations, each indicated as kinetics A to G) while the surface temperatures and the rates of mass loss versus time are plotted in Figure 9 (Q_0 = 50 kW/m^2). The monomer efflux rates at 50% conversion (range of values 1.8-2.2 cm/s) and the maxima (3.8-4.4 cm/s) are not exceedingly different as well as the surface temperature (values in the range 655-776 K), despite of the significant variation in the PMMA degradation kinetics (the activation energies span the wide range 140-280 kJ/mol). However, these variations significantly affect the radiative flame heat flux, resulting from modified radiative properties of the gas phase, with values from 27 kW/m^2 (kinetics F with v_s = 2.1 cm/s) to 18 kW/m^2 (kinetics D with v_s = 1.8 cm/s), and the

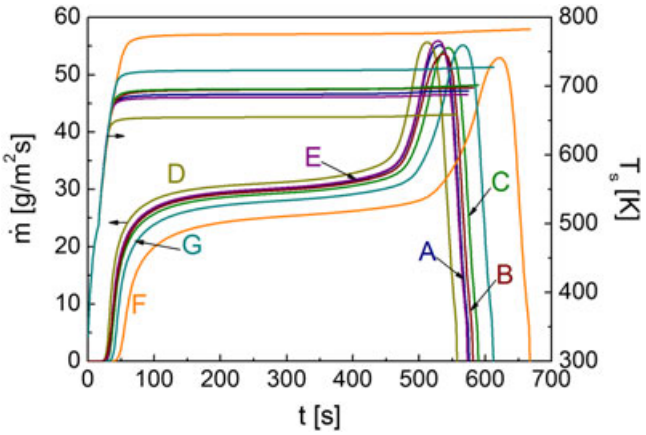

FIGURE 9 Poly(methylmethacrylate) mass loss rate and surface temperature versus time as simulated for the reference case A and with polymer decomposition kinetics as indicated by cases B to G of Table 3 (Q_0 = 50 kW/m^2) [Colour figure can be viewed at wileyonlinelibrary.com]

TABLE 3 Predicted output variables for the solid and gas phases (for the definitions see Table 1) as simulated for the reference case A (kinetics as in Di Blasi[24]) and with polymer decomposition kinetics indicated as B (Madorsky[45]), C (Lehrle et al[46]), D (Hirata et al[47]), E (Madorsky[45]), F (Hirata et al[47]), and G (Arisawa and Brill[48]) for Q_0 = 50 kW/m^2

	Kinetic Parameters		t_{50}, s	T_s, K	v_s, cm/s	t_{max}, s	v_{smax}, cm/s	t_c, s	Q_{rad}, kW/m^2	Q_{cond}, kW/m^2	$Q_{re\text{-}rad}$, kW/m^2	Q_N, kW/m^2	Q_{Nf}, kW/m^2	100 × Q_{Nf} / Q_0	T_{av}, K	T_{max}, K
	A, s^{-1}	E, kJ/mol														
A	1.32 × 10^{13}	188	342	689	2.2	532	4.0	546	22.5	7.0	12.0	67.5	17.5	35.0	717	1862
B	1.96 × 10^{9}	140	345	695	2.2	538	3.9	551	23.2	7.0	12.5	67.7	17.7	35.4	715	1857
C	4.15 × 10^{14}	210	352	696	2.2	545	4.0	559	23.1	7.2	12.6	67.7	17.7	35.4	713	1849
D	2.9 × 10^{16}	220	327	655	1.8	513	3.8	528	17.7	7.6	9.9	65.4	15.4	30.8	718	1867
E	2.89 × 10^{16}	230	341	684	2.2	529	4.0	544	22.2	7.4	11.7	67.9	17.9	35.8	718	1868
F	2.0 × 10^{16}	260	418	776	2.1	622	4.3	637	27.0	7.1	19.4	64.7	14.6	29.2	718	1837
G	1.29 × 10^{19}	280	372	723	2.2	567	4.2	582	22.5	7.2	14.7	65.0	15.0	30.0	715	1842

surface radiative heat losses with values from 19 kW/m^2 (kinetics F with T_s = 776 K) to 10 kW/m^2 (kinetics D with T_s = 655 K). More specifically, high v_s values tend to increase the combustion efficiency and reradiation from the combustion products, which predominates over the increased radiation absorption by the monomer (higher concentrations for both cases). However, higher v_s are also associated with higher T_s and higher surface reradiative heat losses, which largely compensate the above described effect. On the other hand, the conductive heat flux is almost insensitive to the solid decomposition kinetics owing to the approximately unmodified distance of the flame from the solid. Thus, the net flame heat flux varies over a narrow range (15-18 kW/m^2). Finally, it can also be observed that the burn-out times are modified by approximately 20% (the same figure as the v_s variation).

4 | CONCLUSIONS

A detailed unsteady model of the solid-phase processes, coupled with a steady, 2-dimensional computational fluid dynamics model for the gas phase, has been applied to describe the combustion of thick PMMA samples in a cone calorimeter. The first important finding of the study is that a steady coupling between the models for the 2 phases, referred to 50% conversion of the solid phase, produces a solution sufficiently accurate, without the need of applying a dynamic coupling. The agreement between predicted and measured mass loss rates, for cone irradiance levels between 15 and 60 kW/m^2, is acceptable.

An evaluation is provided of the flame heat flux contributions that sum up with the nominal cone value. The radiation absorption/emission properties of the gas phase (vapor fuel and combustion products) play a role of paramount importance in this issue. The fuel vapors, which undergo thermal cracking for temperatures above 773 K, essentially absorb radiation whereas, for the combustion products formed at high temperatures, radiation emission prevails. As a consequence of the increase in the surface temperature and the production rate of vapor phase MMA with the cone irradiance level, the surface radiation losses as well as the flame radiative heat flux increase whereas the conductive flame heat flux tends to decrease following an increased distance of the flame from the degrading surface. The total net contribution of the flame heat flux becomes a successively smaller fraction of the nominal cone irradiance value, with percentages varying from 127% to 28%, for values of the former in the range 15 to 60 kW/m^2, in qualitative agreement with experimental evidence. On the whole, a weak dependence of the total net heat flux on the flame is observed (values of 19-17 kW/m^2), so that it can approximately be considered constant with the cone irradiance level. Finally, the total net flame heat flux is also not highly affected by the solid-phase decomposition kinetics modified according to the literature values.

ACKNOWLEDGEMENTS

This work is part of the activities conducted in the framework of the project COCET "Comportamento di Materiali Compositi in Condizioni Estreme: Alta Temperatura" (PON02_00029_3206086/F1), coordinated by IMAST and funded by the Italian Ministry of Instruction, University and Research (MIUR), the partial support of which is gratefully acknowledged. The authors also express their sincere thanks to Prof JG Quintiere (University of Maryland) and another anonymous reviewer for their helpful advice and constructive criticism.

ORCID

C. Di Blasi http://orcid.org/0000-0001-5499-6251

REFERENCES

1. Babrauskas V. Development of the cone calorimeter—a bench scale heat release apparatus based on oxygen consumption. *Fire MaterFire Mater*. 1984;8:81-95.
2. Babrauskas V, Parker WJ. Ignitability measurements with the cone calorimeter. *Fire Mater*. 1987;11:31-43.
3. Mouritz AP, Gibson AG. *Fire Properties of Polymer Composite Material*. The Netherlands: Springer Dordrecht; 2006.
4. Schartel B, Hull TB. Development of fire-retarded materials. *Interpretation of cone calorimeter data*, *Fire Mater*. 2007;31:327-354.
5. Staggs JEJ. Modelling the effect of solid-phase additives on thermal degradation of solids. *Polym Degrad Stab*. 1999;64:369-377.
6. Staggs JEJ. A simplified mathematical model for the pyrolysis of polymers with inert additives. *Fire Saf J*. 1999;32:221-240.
7. Spearpoint MJ, Quintiere JP. Predicting the burning of wood using an integral model. *Combust Flame*. 2000;123:308-324.
8. Stoliarov SI, Crowley S, Lyon RE, Linteris GP. Prediction of the burning rates of non-charring polymers. *Combust Flame*. 2009;156:1068-1083.
9. Zhang J, Delichatsios MA, Bourbigot S. Experimental and numerical study of the effects of nanoparticles on pyrolysis of polyamide 6 (PA6) nanocomposite in the cone calorimeter. *Combust Flame*. 2009;156:2056-2062.
10. Patel A, Hull RR, Stec AA, Lyon RE. Influence of physical properties on polymer flammability in the cone calorimeter, Polym Adv Technol 2011; 22: 1100–1107.
11. Snegirev AY, Talalov VA, Stepanov VV, Harris JN. A new model to predict pyrolysis, ignition and burning of flammable materials in fire tests. *Fire Saf J*. 2013;59:132-150.
12. Linteris GT, Lyon RE, Stoliarov SI. Prediction of the gasification rate of thermoplastic polymers in fire-like environments. *Fire Saf J*. 2013;60:14-24.
13. Kempel F, Schartel B, Linteris GT, et al. Prediction of the mass loss rate of polymer materials: impact of residue formation. *Combust Flame*. 2012;159:2974-2984.
14. Tsai TH, Li MJ, Shih IY, Jih R, Wong SC. Experimental and numerical study of autoignition and pilot ignition of PMMA plates in a cone calorimeter. *Combust Flame*. 2001;124:466-480.
15. Novozhilov V, Moghtaderi B, Fletcher DF, Kent JH. Computational fluid dynamic modeling of wood combustion. *Fire Saf J*. 1999;27:69-84.
16. Yuen RKK, Yeoh GH, de Vahl DG, Leonardi E. Modeling the pyrolysis of wet wood—II. Three-dimensional cone calorimeter simulation. *Int J Heat Mass Transfer*. 2007;50:4387-4399.
17. Nelson MI, Brindley J, McIntosh A. A mathematical model of ignition in the cone calorimeter. *Combust Sci Tech*. 1995;104:33-54.
18. Di Blasi C, Crescitelli S, Russo G, Cinque G. Numerical model of ignition processes of polymeric materials including gas phase absorption of radiation. *Combust Flame*. 1991;83:333-344.
19. Rhodes BT. Burning rate and flame heat flux for PMMA in the cone calorimeter, NIST-GCR-95-664, National Institute of Standards and Technology, 1994.
20. Rhodes BT, Quintiere JG. Burning rate and flame heat flux for PMMA in a cone calorimeter. *Fire Saf J*. 1996;26:221-240.
21. Hopkins D, Quintiere JG. Material fire properties and predictions for thermoplastics. *Fire Saf J*. 1996;26:241-268.
22. Quintiere JG, Rhodes BT. Fire growth models for materials, NIST-GCR-94-647, National Institute of Standards and Technology,1994.

23. Luche J, Rogaume T, Richard F, Guillame E. Characterization of thermal properties and analysis of combustion behaviour of PMMA in a cone calorimeter. *Fire Saf JFire Saf J*. 2001;46:451-461.
24. Di Blasi C, Galgano A, Branca C. Modeling the thermal degradation of poly(methyl methacrylate)/carbon nanotube nanocomposites. *Polym Degrad Stab*. 2013;98:266-275.
25. Di Blasi C, Galgano A. Influences of properties and heating characteristics on the thermal decomposition of polymer/carbon nanotube nanocomposites. *Fire Saf J*. 2013;59:166-177.
26. Fluent 6.3 User's guide. Copyright © 2006 by Fluent Inc. Centerra Resource Park 10, Cavendish Court, Lebanon , NH 03766, USA.
27. Riviere P, Soufiani A. Updated band model parameters for H2O, CO2, CH4 and CO radiation at high temperature. *Int J Heat Mass Transfer*. 2012;55:3349-3358.
28. Park SH, Stretton AS, Tien CL. Infrared radiation properties of methyl methacrylate vapor. *Comb Sci Tech*. 1988;62:257-271.
29. Zeng WR, Li SF, Chow WK. Review on chemical reactions of burning poly(methyl methacrylate) PMMA, J Fire Sci 2002; 20: 401–433.
30. Di Blasi C. Predictions of wind-opposed flame spread rates and energy feedback analysis for charring solids in a microgravity environment. *Combust Flame*. 1995;100:332-340.
31. Di Blasi C. Modeling of solid and gas phase processes during composite material degradation. *Polym Degrad Stab*. 1996;54:241-248.
32. Galgano A, Di Blasi C, Horvat A, Sinai Y. Experimental validation of a coupled solid- and gas-phase model for combustion and gasification of wood logs. *Energy Fuel*. 2006;20:2223-2232.
33. Galgano A, Di Blasi C. Coupling a CFD code with a solid-phase combustion model. *Progress in Computational Fluid Dynamics*. 2006;6:287-302.
34. Linteris G, Zammarano M, Wilthan B, Hanssen L. Absorption and reflection of infrared radiation by polymers in fire-like environments. *Fire Mater*. 2012;36:537-553.
35. Bal N, Rein G. Numerical investigation of the ignition delay time of a translucent solid at high radiant heat fluxes. *Combust Flame*. 2011;158:1109-1116.
36. Galgano A, Branca C, Di Blasi C, Vollaro P, Milella E. Modeling the ignition of poly(methyl methacrylate)/carbon nanotube nanocomposites. *Polym Degrad Stab*. 2017;144:344-353.
37. Perry RH, Green DW, Maloney JO (Eds). *Perry's Chemical Engineers' Handbook*. 6th ed. New York: McGraw-Hill; 1984.
38. Zhou Y, Yang L, Dai J, Wang Y, Deng Z. Radiation attenuation characteristics of pyrolysis volatiles of solid fuels and their effect for radiant ignition model. *Combust Flame*. 2010;157:167-175.
39. Beaulieu PA, Dembsey NA. Effect of oxygen on flame heat flux in horizontal and vertical orientations. *Fire Saf J*. 2008;43:410-428.
40. Pizzo Y, Lallemand C, Kacem A, et al. Steady and transient pyrolysis of thick clear PMMA slabs. *Combust Flame*. 2015;162:226-236.
41. Li J, Gong J, Stoliarov SI. Gasification experiments for pyrolysis model parameterization and validation. *Int J Heat Mass Transfer*. 2014;77:738-744.
42. Di Blasi C, Branca C. A mathematical model for the non-steady decomposition of intumescent coatings. *AIChE J*. 2001;47:2359-2370.
43. Di Blasi C. Influences of model assumptions on the predictions of cellulose pyrolysis in the heat transfer controlled regime. *Fuel*. 1996;75:58-66.
44. Holland BJ, Hay JN. The effect of polymerisation conditions on the kinetics and mechanisms of thermal degradation of PMMA. *Polym Degrad Stab*. 2002;77:435-439.
45. Madorsky SL. Rates and activation energies of thermal degradation of styrene and acrylate polymers in a vacuum. *J Polym Sci A*. 1953;11:491-506.
46. Lehrle RS, Peakman RE, Robb JC. Pyrolysis-GLC utilised for a kinetic study of the mechanisms of initiation and termination in the thermal degradation of polystyrene. *Eur Polym JEur Polym J*. 1982;18:517-529.
47. Hirata T, Kashiwagi T, Brown JE JE. Thermal and oxidative degradation of poly(methyl methacrylate): weight loss. *Macromolecules*. 1985;18:1410-1418.
48. Arisawa H, Brill TB. Kinetics and mechanisms of flash pyrolysis of poly(methyl methacrylate) (PMMA). *Combust Flame*. 1997;109:415-426.

How to cite this article: Galgano A, Di Blasi C, Branca C. Numerical evaluation of the flame to solid heat flux during poly(methyl methacrylate) combustion. *Fire and Materials*. 2018;1–10. https://doi.org/10.1002/fam.2505